E14-2014-80

E. Uyanga [1,2,*], G. Sevjidsuren [1], P. Altantsog [1], D. Sangaa [1]

THE STRUCTURAL STUDY OF ALTERNATIVE SUPPORT MATERIALS FOR **PEMFC**

[1] Institute of Physics and Technology, Mongolian Academy of Sciences, Ulaanbaatar, Mongolia
[2] Joint Institute for Nuclear Research, Dubna
[*] E-mail: uyanga@jinr.ru

Уянга Э. и др.   Е14-2014-80

Структурные исследования альтернативных материалов
для протонно-обменных топливных элементов (PEMFC)

Проведены синтез и исследование легированного ниобием мезопористого оксида титана TiO_2, который используется как поддерживающий материал катализатора катода в топливных элементах с полимерным мембранным электролитом (PEMFC). Синтез $Nb_xTi_{1-x}O_2$ (далее NTO) был выполнен двумя различными методами: 1) поверхностным осаждением при комнатной температуре (для $x = 0{,}1$ и $0{,}005$), 2) твердофазной реакцией при 700 и 1000 °C (для $x = 0{,}1$). Рентгенодифракционный анализ показал, что синтезированные порошки содержат только структурные TiO_2 фазы — анатаз и рутил. Дифракционные пики, принадлежащие соединениям Nb, отсутствовали, что свидетельствует о внедрении Nb в структуру этих фаз. Эксперименты по дифракции рентгеновских лучей и по комбинационному рассеянию света показали, что легирование Nb препятствует фазовому переходу анатаз–рутил. Внедрение наночастиц в мезопористый материал NTO с использованием методики полиола происходит равномерно, что следует из наблюдений с помощью сканирующей электронной микроскопии (SEM). Для выяснения роли Nb в блокировании фазового перехода анатаз–рутил были проведены XAS эксперименты на краях поглощения Nb и Ti (K-край). Из этих данных следует, что ионы ниобия находятся в наноструктурированном TiO_2 в зарядном состоянии $+5$.

Работа выполнена в Лаборатории нейтронной физики им. И. М. Франка ОИЯИ.

Uyanga E. et al.   Е14-2014-80

The Structural Study of Alternative Support Materials for PEMFC

Mesoporous niobium-doped titanium oxide (NTO) was synthesized and investigated as a cathode catalyst support material for polymer electrolyte membrane fuel cells (PEMFC). We prepared the NTO support by two different methods: 1) room-temperature synthesis of $Nb_xTi_{1-x}O_2$ ($x = 0.1$, 0.005) via surfactant templating and 2) high-temperature synthesis (700 and 1000 °C) of $Nb_xTi_{1-x}O_2$ ($x = 0.1$). The XRD analysis revealed only the presence of anatase and rutile TiO_2 phase in the synthesized support powder. The existence of any peaks belonging to Nb compounds was not observed, indicating that Nb is incorporated in the lattice. The X-ray diffraction and Raman scattering measurements revealed anatase-to-rutile phase transition hindering due to Nb doping. Pt nanoparticles were dispersed in the mesoporous NTO support by the polyol method and characterized by the scanning electron microscopy. The Pt particle sizes, interatomic distances, and distribution were found by XRD, XAS, and SEM. To better understand the role played by the dopant atoms in inhibiting both phase transformation to rutile and grain growth, XAS measurements were performed at the Nb K and Ti K absorption edges. The XAS analysis results indicate that niobium atoms are incorporated into nanostructured TiO_2 with $+5$ valence state.

The investigation has been performed at the Frank Laboratory of Neutron Physics, JINR.

1. INTRODUCTION

Carbon type materials (e. g., Vulcan XC-72) are typical catalyst support materials for PEMFCs due to their large surface area, high electrical conductivity and well-developed pore structure. However, corrosion of the carbon supports was observed under PEMFC operating conditions. The electrochemical corrosion of the carbon support causes agglomeration and sintering of the Pt catalyst particles, resulting in a decreased electrochemical surface area of the catalyst. These effects result in a rapid degradation of the Pt catalyst and thus shorten the lifetime of PEMFC, which is limiting for most of its projected applications. This problem has initiated a lot of research in the last few years aimed at finding an appropriate replacement for carbon supports [1–4].

Titanium dioxide (TiO_2) is a widely used material with a variety of potential applications in catalysis, photovoltaics, water splitting and gas sensors. TiO_2 possesses good mechanical resistance and stability in acidic and oxidative environments. These properties suggest that TiO_2 may be considered as an alternative catalyst support. However, its low electrical conductivity prevents its use in fuel cells. TiO_2 exists in three crystalline forms: the most common types are rutile and anatase. Among three phases, rutile is thermodynamically stable at high temperatures. Anatase and brookite crystalline structures undergo a phase transition above $600\,°C$ and are converted into rutile crystalline phase. The anatase phase of titania is usually stabilized by cation addition. It is desirable for fuel cell catalysts due to a better catalytic activity for oxidizing organic compounds compared to the rutile and brookite structures.

For the latter, niobium seems to be a very promising doping species in TiO_2 which according to a number of previous reports [5, 6] gives rise to shallow donor states mostly attributed to mixed Nb4d–Ti3d states located 0.02–0.03 eV below the conduction-band minimum. These states can be ascribed to substitutional doping in TiO_2, resulting in an increase of electron conductivity. Moreover, doping of TiO_2 with Nb slows down the anatase-to-rutile phase transformation preventing growth of the particles, and that might lead to the enhancement of the specific surface area of the catalyst support [7–8].

Recently, S. Y. Huang et al. [1] showed that the conductivity of Nb-doped anatase (synthesized via a template-assisted method) increases with temperature.

However, the rutile phase was observed above $600\,^{\circ}\text{C}$ and the particle sizes increased rapidly (the particle size of the rutile phase is always larger than that of the anatase). Consequently, the active phase and particle size are the important parameters that influence catalytic activity, stability, specific surface, etc., which are the main properties of the TiO_2 support. In this work, we focus on the preparation of a thermally stable, mesoporous anatase support for the electrocatalyst and determine the structure of the catalyst by temperature-dependent (700 and $1000\,^{\circ}\text{C}$) X-ray diffraction, absorption and Raman scattering studies.

2. EXPERIMENTAL

2.1. Preparation of $Nb_xTi_{1-x}O_2$ (NTO) Support. High-temperature synthesis: NbO_2 and TiO_2 sintered at high temperatures to form NTO support were synthesized through the modified sol-gel procedure proposed by Fuentes *et al.* [9]. The samples were prepared using titanium IV butoxide, niobium ethoxide and Cetyl trimethylammonium bromide (CTAB). The precursors were mixed by magnetic stirring in hydrochloric acid and ethanol. The relative amounts of Nb:Ti were chosen to produce a material with the required stoichiometry. The resulting solid was transferred to the solution of DI water and NH_4OH under continuous stirring and kept for 48 h. The sample was calcined at $400\,^{\circ}\text{C}$ for 2 h. The sample was further calcined at 700 and $1000\,^{\circ}\text{C}$ for 2 h.

The room-temperature synthesis route for NTO via a surfactant templating method was described by Garcia *et al.* [5]. NTO was prepared using titanium IV butoxide, niobium ethoxide, and octadecylamine. The precursors were mixed by magnetic stirring in dehydrated ethanol. Next, deionized water was added to the solution, and the gel was aged for 48 h. The resulting gel was filtered and dried at $100\,^{\circ}\text{C}$ in a vacuum oven for 12 h.

2.2. Synthesis of $Pt/Nb_xTi_{1-x}O_2$ Electrocatalyst. Pt was deposited by the polyol method. 200 mg of the NTO powder was suspended in 60 ml of ethylene glycol and dispersed by sonication. The second solution of 100 mg hexachloroplatinate ($H_2PtCl_6 \cdot 6H_2O$) dissolved in 10 ml ethylene glycol was prepared and added drop-wise to the first solution under stirring. After stirring for 30 minutes,

Table 1. Pt supported on NTO catalysts, prepared by different synthesis methods

Samples	Preparation	Heating temperature, $^{\circ}\text{C}$
A $Pt/Nb_{0.1}Ti_{0.9}O_2$	Sol-gel	700
B $Pt/Nb_{0.1}Ti_{0.9}O_2$		1000
C $Pt/Nb_{0.1}Ti_{0.9}O_2$	Low-temperature surfactant-templating method	—
D $Pt/Nb_{0.005}Ti_{0.995}O_2$		—

the solution was heated to $140\,°C$ for 3 h under reflux. Finally, when the solution was cooled down, it was filtered and dried at $80\,°C$ overnight. Table 1 shows details of the catalust synthesis.

2.3. Characterization Measurement. The X-ray data were collected between 20 and 90 (2θ) at room temperature using a Philips X'PERT PRO MRD using step sizes of 0.08 and 30 s of counting time. The measured diffraction patterns were refined by the Rietveld method using the MAUD software.

The Raman spectra were recorded using an Yvon Jobin Horiba (XploRA) spectrometer. The measurement was performed with a diode laser source (785 nm) and an incident power of 40 mW.

X-ray absorption spectroscopy (XAS) at Pt L_3-edge was done at beam lines BL07A of the National Synchrotron Radiation Research Center, Hsinchu, Taiwan [10]. The data fitting was done using the software package IFEFFIT.

The morphology of the catalyst was examined by scanning electron microscopy (SEM) using a high-resolution thermally aided field emission SEM (Zeiss, LEO 1530 Gemini).

3. RESULTS AND DISCUSSION

3.1. XRD and Raman Measurements of the Synthesized Catalyst. Figure 1, a shows the XRD patterns of Pt supported on the NTO catalysts. In all XRD patterns, sharp well-defined peaks of the Pt nanopaticles can be detected. The diffraction reflections for both the anatase and the rutile phase are observed in sample A, B. Additionally, the spectrum reveals small peaks representing titanium niobium oxide ($TiNb_2O_7$) that are usually seen in the samples treated at
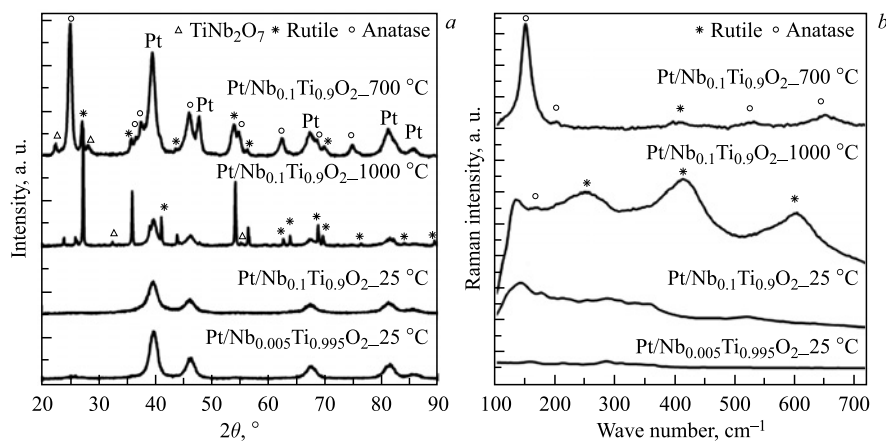

Fig. 1. X-ray diffraction patterns (a) and Raman spectra (b) of Pt/Nb doped TiO_2

3

high temperatures [9]. No niobium oxide phases were detected in the sample. The refined lattice parameters of anatase are a = 3.797 Å and c = 9.533 Å at sample B. These values are higher compared with those of pure anatase (JCPDS 21-1272) indicating that niobium substitutionally replaces some Ti sites in the lattice of the TiO_2 structure.

The XRD patterns of sample A show the mixture of anatase (66.7 wt. %) and rutile (15.2 wt. %) phases. It confirms that Nb doping prevents the anatase-to-pure-rutile phase transformation. The diffraction patterns of sample B reveal the most intense peak of the rutile (76.7 wt. %) phase. In the XRD patterns of the room temperature synthesis, weaker anatase and rutile peaks appear at 25.3° and 54.5°, respectively. The XRD analysis results of particle sizes are presented in Table 2. It is well known that the particle size is a crucial factor for the catalytic activity of a catalyst support. It has been found that the rutile and anatase particle sizes of Pt/NTO calcined at 700 °C are much smaller than those of the sample after calcination at 1000 °C.

Table 2. Fit results of XRD patterns for Pt supported NTO catalysts

Synthesized samples	Particle size, nm			R_{wp}, %
	Platinum	Anatase	Rutile	
A Pt/Nb$_{0.1}$Ti$_{0.9}$O$_2$	10.7	20.3	26.6	9.4
B Pt/Nb$_{0.1}$Ti$_{0.9}$O$_2$	10.0	119.8	258.8	12.3
C Pt/Nb$_{0.1}$Ti$_{0.9}$O$_2$	5.8	—	—	11.4
D Pt/Nb$_{0.005}$Ti$_{0.995}$O$_2$	8.5	—	—	10.9

The evolution of Raman spectra for Pt/NTO electrode is shown in Fig. 1, *b*. The qualitative phase composition of the samples obtained from the XRD studies was confirmed by the Raman spectra. In the Raman spectra of sample A the strongest band of anatase appears at 149 cm^{-1}, weaker bands can be detected at 202, 396, 531, and 649 cm^{-1} [11], and rutile peaks are observed at 237 and 410 cm^{-1}. Comparing the reference Raman spectra, it is clear that the bands shift towards higher wave numbers. The Raman shifts observed are due to the doping and temperature. In the case of sample B, the Raman bands of rutile phase are observed at 251, 416, and 598 cm^{-1} [12], and a small anatase peak appears at 168 cm^{-1}. The strong background signals in the Raman spectra of sample C are from amorphous TiO_2. The Raman scattering results of samples C, D correspond to amorphous TiO_2.

3.2. XAS Measurements. The normalized Nb K-edge spectra of high-temperature synthesized Pt/NTO electrodes are presented in Fig. 2, *a*. The XANES spectra of TiO_2 samples doped with Nb are almost identical. The absorption of the XANES region is related to the site symmetry, coordination, and the oxidation

states of the central atoms. The Nb K-edge XANES spectra arise from $1s-4d$ electronic transition and are characterized by a weak pre-edge absorption shoulder at 19895 eV [13]. This weak pre-edge absorption shoulder is also visible in the XANES spectra of reference compound Nb_2O_5, indicating that Nb ions are dispersed in the titanium dioxide with oxidation state $+5$. The pre-edge absorption shoulder can be reasonably associated with the presence of a distorted coordination environment of the Nb atoms. The analogy between the absorption shoulder of Nb_2O_5 and Nb-doped titania XANES spectra suggests that in high-temperature synthesized samples, the Nb atoms are located in distorted octahedral sites.

In order to maintain the equilibrium of charges, the extrapositive charge due to Nb^{5+} may be compensated by the creation of an equivalent amount of Ti^{3+} ions, or by the presence of vacancies in the cation sites. Figure $2, b$ shows the Ti K-edge XANES spectra of samples A, B and reference spectra of TiO_2 rutile and anatase. The spectrum of sample A is very similar to the spectra of the reference anatase sample; the spectrum of sample B is similar to those of rutile. No other formations of titania were observed in the XANES spectra, which suggests that charge compensation of our samples is achieved by the formation of Ti vacancies. A Ti K-edge XANES spectrum is usually divided into two regions. The region above approximately 4980 eV is assigned to the well-understood dipole-allowed $1s \rightarrow np\,(n \geqslant 4)$ transitions; the so-called pre-edge peaks lie below 4980 eV [14]. The XANES spectrum at the Ti K-edge shows several well-defined pre-edge peaks. The Pt/NTO electrodes gave three small pre-edge peaks named A_1, A_3, and B (Fig. 2, b) which can be assigned to the octahedrally coordinated titanium atoms of anatase and rutile with high crystallite. These pre-edge peaks correspond to $1s$ transitions to the t_{2g} and e_g bands, which arise dominantly from the hybridization of Ti $3d$ and $4p$ orbitals on different sites in
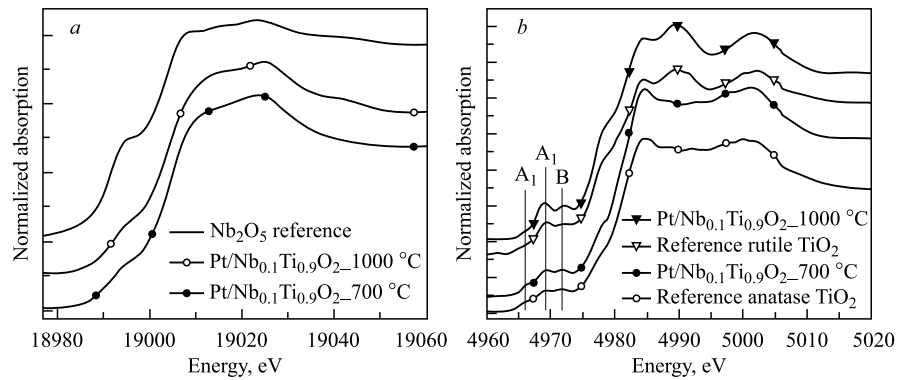

Fig. 2. Normalized Nb K-edge XANES spectra (a) and normalized Ti K-edge XANES spectra (b) of samples A and B

the conduction band region [15]. The position of the pre-edge peaks from the Pt/NTO electrodes is very close to that of the reference anatase and rutile. This is clear evidence that Ti is present as Ti^{4+} and in a six-fold coordinated site.

Figure 3, a shows the XANES region of the spectra at the Pt L_3-edge for Pt/NTO electrodes. All catalysts appear significantly oxidized as indicated by their pronounced white-line intensities and show a spectrum very similar to that of the bulk metallic platinum reference foil. The metallic spectrum exhibits two bands at 11581 and 11595 eV immediately after the white-line region.

The parameter N is 12 in typical bulk fcc structures, but decreases as the surface-to-volume atomic ratio increases [16]. For small particles, the average first
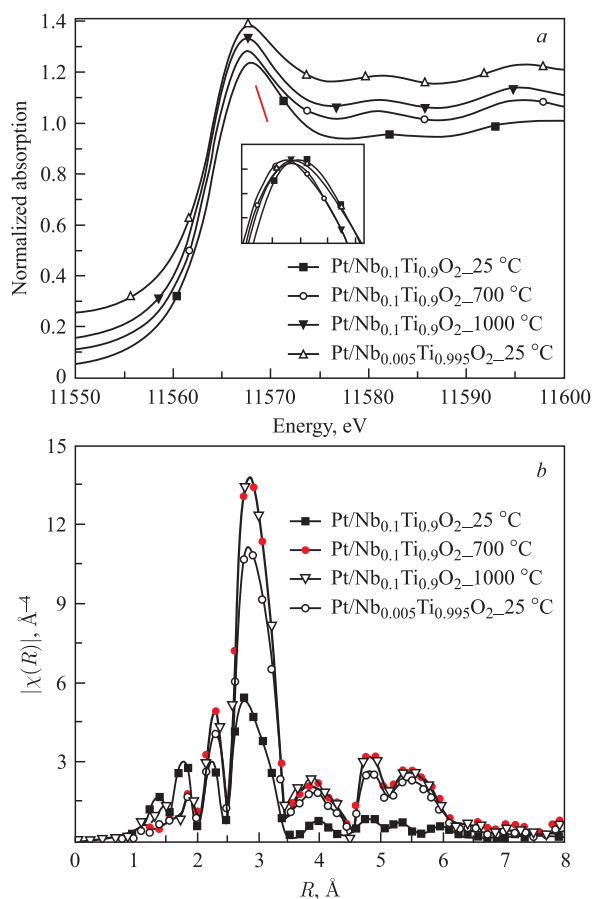

Fig. 3. XANES spectra at Pt L_3-edge for various samples (a). Fourier transformed EXAFS spectrum of 14 wt. % Pt/Nb_xTi$_{1-x}$O$_2$ measured at the Pt L_3-edge (11564 eV) (b)

Table 3. Structural data obtained using XAS analysis at the Pt L$_3$-edge

Synthesized samples	Bonds	R, [Å]	N	σ^2, [Å^2]
A Pt/Nb$_{0.1}$Ti$_{0.9}$O$_2$	Pt–Pt	2.758	8.9	0.0012
B Pt/Nb$_{0.1}$Ti$_{0.9}$O$_2$	Pt–Pt	2.759	9.3	0.0014
C Pt/Nb$_{0.1}$Ti$_{0.9}$O$_2$	Pt–Pt	2.741	5.9	0.0044
D Pt/Nb$_{0.005}$Ti$_{0.995}$O$_2$	Pt–Pt	2.756	8.6	0.0035

Note. R–interatomic distances, N — coordination number, σ^2 — Debay–Waller factor.

shell coordination number is reduced, as the atoms on the particle surface do not have the full number of neighbors. The surface-to-volume ratio and the number of distorted sites at the surface increase as the particle size decreases, a reduction in the magnitude of the FT peaks of nanoparticles is generally observed [17]. In Fig. 3, it can be seen that the main features of the spectra of the Pt nanoparticles show variation with a decrease in the particle size. Thus, we can say that sample C has the smallest particle size compared with other samples. It is confirmed by the XRD analysis results (Table 2) and XAS fitting results (Table 3). All Pt L$_3$-edge EXAFS data were fitted using a least-squares process in the Artemis program, which is a subroutine of IFEFFIT. The fit used only the first shell analysis Pt–Pt scattering path.

A summary of the EXAFS fitting is provided in Table 3 for Pt nanoparticles in the indicated electrodes. No major changes in the Pt bond distance (R) are observed as a function of potential or electrolyte. The Pt–Pt distances are 2.76 Å at high-temperature synthesis, which are similar to that of the bulk platinum. At room-temperature synthesis, the fit shows that the Pt–Pt distances are 2.74 and 2.75 Å, which are smaller than that of the bulk platinum. These indicate that the platinum cluster decreases. The coordination numbers are correlated with the particle sizes, which correspond to the particle size of sample C, smaller than for other electrodes. The coordination number of 9.3 for sample B indicates the presence of large platinum particles.

3.3. Catalyst Characterization by SEM. Figure 4 shows SEM images of the electrodes used in this work. The same Pt precursor solution was used to load Pt onto the various supports. Figure 4, *a–d*, gives the SEM images of sample A, B, C, and D, respectively.

As can be seen from Fig. 4, the Pt/NTO electrodes clearly show the mesoporous character. As shown in Fig. 4, *a*, Pt particles are homogeneously dispersed on the NTO support surface. On the support of sample B the Pt nanoparticles were agglomerated, resulting in an inhomogeneous distribution (Fig. 4, *b*). In contrast, no apparent Pt nanoparticles could be identified in Fig. 4, *c* and *d*, presumably
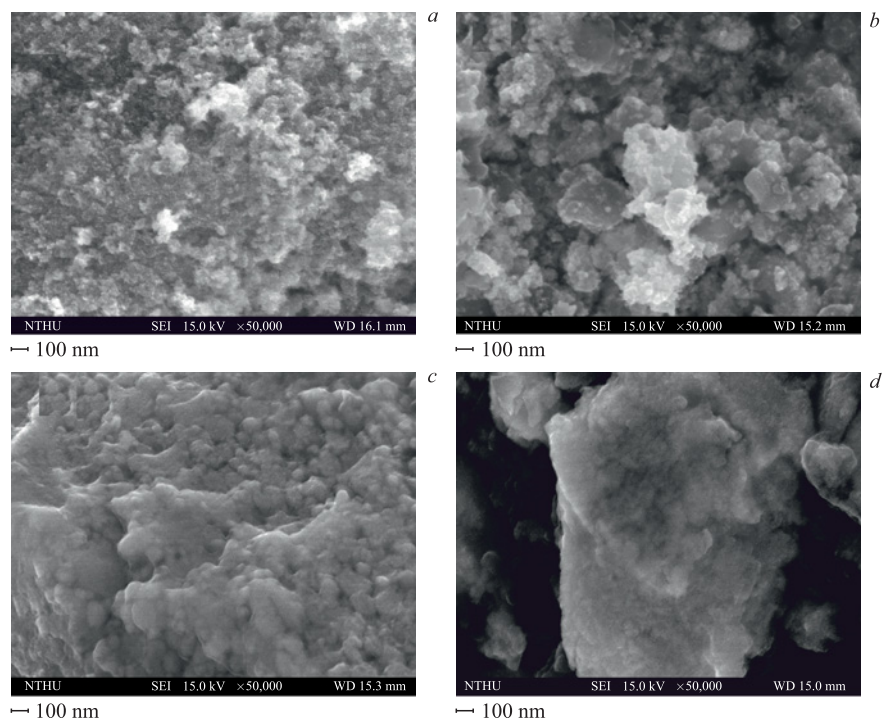
Fig. 4. SEM images of sample A (*a*), sample B (*b*), sample C (*c*), and sample D (*d*)

because the nanoparticles of sample C and D were the smallest compared with those of other samples and thus invisible under SEM imaging.

4. CONCLUSIONS

This work presents the preparation of mesoporous Nb-doped TiO_2 support materials by two chemical methods and their characterization by XRD, Raman, XAS, and SEM. The NTO support Pt catalysts were successfully prepared using the polyol method and characterized by the SEM technique.

The XRD and Raman results for Pt/ $Nb_{0.1}Ti_{0.9}O_2$ catalysts, which were synthesized at high temperatures, indicate the presence of anatase, rutile and their absence in niobium oxide structures. Nb doping has been confirmed by the XRD and XAS measurement results. The addition of niobium during the synthesis stabilized the anatase form of TiO_2, which is confirmed by the main anatase structure (66.7 wt. %) observed at $700\,^{\circ}$C calcination temperature. The transformation of anatase into rutile at high temperatures is more kinetically hindered by

Nb doping. We observed Nb ions segregated from the grains, forming $TiNb_2O_7$ oxidized species at $1000\,°C$ calcinations. Amorphous TiO_2 was observed in the XRD, Raman patterns of sample C and D.

The platinum particle sizes of the high-temperature synthesis were higher than those of the room-temperature synthesis. The shell coordination number of the XAS measurement confirmed the results of the particle sizes of the XRD refinement. As determined by the Rietveld refinement for $Pt/Nb_{0.1}Ti_{0.9}O_2$ catalysts calcined at $700\,°C$, the particle size of anatase is 20.3 nm and that of rutile is 26.6 nm.

The XAS spectra as compared with the standard compounds show that Nb atoms are dispersed in TiO_2 crystal structure as Nb^{5+}, which may be ascribed to the charge compensating defects introduced by one Ti vacancy per four Nb^{5+}.

Consequently, among our prepared four samples, $Pt/Nb_{0.1}Ti_{0.9}O_2$ powder heat treated at $700\,°C$ was selected for further electrochemical investigation due to its mesoporous structure, stability at high temperatures, optimum particle size and good dispersivity of Pt nanoparticles, which are required for a material serving as a catalyst support for PEMFC applications. The sol-gel method combined with high-temperature calcination is considered to be a promising technique for Nb-doped TiO_2.

REFERENCES

 1. *Huang S. Y., Ganesan P., Popov N. B. //* Appl. Catal. B. 2010. V. 96. P. 224–231.
 2. *Park K. W., Seol K. S. //* Electrochem. Commun. 2007. V. 9. P. 2256–2260.
 3. *Huang S. Y. et al. //* J. Am. Chem. Soc. 2009. V. 131. P. 13898–13899.
 4. *Elezovic N. R. et al. //* Electrochim. Acta. 2010. V. 56. P. 9020–9026.
 5. *Garcia B. L., Fuentes R., Weidner J. W. //* Electrochem. Solid. State. Lett. 2007. V. 10. P. B108–B110.
 6. *Chhina H.* PhD Thesis: University of Toronto, 2009.
 7. *Ettingshausen F. et al. //* ECS Trans. 2009. V. 25. P. 1883–1892.
 8. *Elezovic N. R. //* J. Power Sources. 2010. V. 195. P. 3961–3968.
 9. *Fuentes R., Garcia B. L., Weidner J. W. //* J. Electrochem. Soc. 2011. V. 158. P. B461–B466.
10. *Chang S. H. //* Chinese J. Phys. 2012. V. 50. P. 220
11. *Coi H. Ch., Jung Y. M., Kim S. B. //* Vib. Spectrosc. 2005. V. 37. P. 33–38.
12. *Mei B. //* J. Mater. Chem. 2011. V. 21. P. 11781–11790.

13. *Sacerdoti M. et al. //* J. Solid State Chem. 2004. V. 177. P. 1781–1788.
14. *Lee Y. et al. //* Res. Chem. Intermed. 2003. V. 29. P. 783.
15. *Choi H. Ch. et al. //* Appl. Spectrosc. 2004. V. 58. P. 598–602.
16. *Principi E. et al. //* Phys. Chem. Chem. Phys. 2009. V. 11. P. 9987–9995.
17. *Liu D. G., Lee J. F., Tang M. Ts. //* J. Mol. Catal. A-Chem. 2005. V. 240. P. 197–206.

Редактор *Э. В. Ивашкевич*